

A TIME-ACCURATE FINITE VOLUME METHOD VALID AT ALL FLOW VELOCITIES

S.-W. Kim
Resident Research Associate
CFD for Space Branch,
NASA Lewis Research Center, MS 5-11,
Cleveland, Ohio 44135

535-34

~~43810~~

p. 31

A finite volume method to solve the Navier-Stokes equations at all flow velocities (e.g., incompressible, subsonic, transonic, supersonic and hypersonic flows) is presented. The numerical method is based on a finite volume method that incorporates a pressure-staggered mesh and an incremental pressure equation for the conservation of mass. Comparison of three generally accepted time-advancing schemes, i.e., Simplified Marker-and-Cell (SMAC), Pressure-Implicit-Splitting of Operators (PISO), and Iterative-Time-Advancing (ITA) scheme, are made by solving a lid-driven polar cavity flow and self-sustained oscillatory flows over circular and square cylinders. Calculated results show that the ITA is the most stable numerically and yields the most accurate results. The SMAC is the most efficient computationally and is as stable as the ITA. It is shown that the PISO is the most weakly convergent and it exhibits an undesirable strong dependence on the time-step size. The degenerated numerical results obtained using the PISO is attributed to its second corrector step that cause the numerical results to deviate further from a divergence free velocity field. The accurate numerical results obtained using the ITA is attributed to its capability to resolve the nonlinearity of the Navier-Stokes equations.

The present numerical method that incorporates the ITA is used to solve an unsteady transitional flow over an oscillating airfoil and a chemically reacting flow of hydrogen in a vitiated supersonic airstream. The turbulence fields in these flow cases are described using multiple-time-scale turbulence equations.

For the unsteady transitional over an oscillating airfoil, the fluid flow is described using ensemble-averaged Navier-Stokes equations defined on the Lagrangian-Eulerian coordinates. It is shown that the numerical method successfully predicts the large dynamic stall vortex (DSV) and the trailing edge vortex (TEV) that are periodically generated by the oscillating airfoil. The calculated streaklines are in very good comparison with the experimentally obtained smoke picture. The calculated turbulent viscosity contours show that the transition from laminar to turbulent state and the relaminarization occur widely in space as well as in time. The ensemble-averaged velocity profiles are also in good agreement with the measured data and the good comparison indicates that the numerical method as well as the multiple-time-scale turbulence equations successfully predict the unsteady transitional turbulence field.

The chemical reactions for the hydrogen in the vitiated supersonic airstream are described using 9 chemical species and 48 reaction-steps. Consider that a fast chemistry can not be used to describe the fine details (such as the instability) of chemically reacting flows while a reduced chemical kinetics can not be used confidently due to the uncertainty contained in the reaction mechanisms. However, the use of a detailed finite rate chemistry may make it difficult to obtain a fully converged solution due to the coupling between the large number of flow, turbulence, and chemical equations. The numerical results obtained in the present study are in good agreement with the measured data. The good comparison is attributed to the numerical method that can yield strongly converged results for the reacting flow and to the use of the multiple-time-scale turbulence equations that can accurately describe the mixing of the fuel and the oxidant.

PRECEDING PAGE BLANK NOT FILMED

**A TIME-ACCURATE FINITE VOLUME METHOD VALID AT
ALL FLOW VELOCITIES**

S.-W. Kim*

**CFD for Space Branch,
NASA Lewis Research Center, MS 5-11,
Cleveland, Ohio 44135**

*** Resident Research Associate**

CONTENTS

- I. Introduction.
- II. Comparison of Unsteady Flow Solution Techniques.
Iterative Time-Advancing Scheme (ITA).
Simplified Marker and Cell (SMAC).
Pressure-Implicit Splitting of Operators (PISO).
- Example Flows.
Lid-driven polar cavity flow starting from rest.
Flow over a circular cylinder.
Flow over a square cylinder.
- III. Application of the Iterative Time-Advancing Scheme (ITA),
Unsteady Transitional Flow over Oscillaing Airfoil,
Combustion of H₂ in Vitiated Supersonic Airstream.
- VI. Conclusions and Discussion.

INTRODUCTION

Fluid flow inside Space Propulsion Systems includes all flow velocities, i.e.,

Incompressible Flows ($M < \epsilon$),
Low Mach Number Flows,
Transonic Flows,
Supersonic Flows, and
Hypersonic Flows.

A number of numerical methods to solve flows (mostly steady flows) at all flow velocities have been proposed in recent years.

Establish a numerical method that will yield accurate numerical results for flows at all velocities that include:

- i. steady and unsteady flows*,
- ii. laminar, transitional, and turbulent flows,*
- iii. chemically reacting flows*

* Need to identify a best time-integration scheme among many available methods.

** Multiple-time-scale turbulence equations are used in the present unsteady transitional flow and the chemically reacting flow calculations.

Comparison of Unsteady Flow Solution Techniques*

Iterative Time-Advancing Scheme (ITA).

Simplified Marker and Cell (SMAC).

Pressure-Implicit Splitting of Operators (PISO).

* Kim & Benson, Computers and Fluids, vol. 21, pp. 435-454, 1992

1. Iterative Time-Advancing Scheme (ITA)

Solve momentum equation.

$$(\rho C_1 + A_i) u_i^{***} = \sum_{nb} A_k u_k^{**} + S_i^* - \frac{\partial p^*}{\partial x_i} + \rho C_2 u_i^{n-1} - \rho C_3 u_i^{n-2} \quad (1)$$

Correct the velocity field to be divergence free

Incremental pressure equation

$$\frac{\partial}{\partial x_j} \left\{ \frac{1}{(\rho C_1 + A_j^*)} \frac{\partial p'}{\partial x_j} \right\} = \frac{\partial u_j^{**}}{\partial x_j} \quad (2)$$

Incremental velocity equation

$$u_i' = \frac{1}{(\rho C_1 + A_i^*)} \frac{\partial p'}{\partial x_i} \quad (3)$$

Velocity and pressure corrections

$$u_i^{***} = u_i^{**} + u_i' \quad (4)$$

$$p^{**} = p^* + p' \quad (5)$$

Solve eqs. (1-5) iteratively until all flow variables converge for each time-level.

The ITA can account for the nonlinearity in each component of the momentum equations and the nonlinear coupling of u- and v-velocity.

2. Simplified Marker and Cell (SMAC)

Predictor Step: Solve momentum equation.

$$(\rho C_1 + A_1^{n-1})u_j^* = \sum_{nb} A_k^{n-1} u_k^* + S_1^{n-1} - \frac{\partial p^{n-1}}{\partial x_j} + \rho C_2 u_1^{n-1} - \rho C_3 u_1^{n-2} \quad (1)$$

Corrector Step: Correct the velocity field to be divergence free

Auxiliary pressure potential equation

$$\frac{\partial}{\partial x_j} \left(\frac{\partial \phi}{\partial x_j} \right) = \frac{\partial u_j^*}{\partial x_j} \quad (2)$$

Update velocity

$$u_1^n = u_1^* - \frac{\partial \phi}{\partial x_1} \quad (3)$$

Consistent pressure field

$$p^n = p^{n-1} + \rho C_1 \phi \quad (4)$$

Solve eqs. (1-4) for each time-level. The velocity field strongly satisfy the conservation of mass.

Conservation of momentum is achieved by obtaining a consistent pressure field.

3. Pressure-Implicit Splitting of Operators

Predictor Step: Solve momentum equation.

$$(\rho C_1 + A_1^{n-1}) u_j^* = H_i^* - \frac{\partial p^{n-1}}{\partial x_j} + \rho C_2 u_1^{n-1} - \rho C_3 u_1^{n-2} \quad (1)$$

where

$$H_i^* = \sum_{nb} A_k^{n-1} u_k^* + S_1^{n-1}$$

First Corrector Step: Correct velocity and pressure for mass imbalance

Incremental pressure equation

$$\frac{\partial}{\partial x_j} \left\{ \frac{1}{(\rho C_1 + A_1^{n-1})} \frac{\partial p'}{\partial x_j} \right\} = \frac{\partial u_j^*}{\partial x_j} \quad (2)$$

Correct velocity and pressure

$$u_i' = - \frac{1}{(\rho C_1 + A_1^{n-1})} \frac{\partial p'}{\partial x_i} \quad (3)$$

$$u_i^{**} = u_i^* + u_i' \quad (4)$$

$$p^{**} = p^* + p' \quad (5)$$

Second Corrector Step: Correct velocity and pressure for momentum imbalance

Incremental pressure equation

$$\frac{\partial}{\partial x_j} \left\{ \frac{1}{(\rho C_1 + A_j^{**})} \frac{\partial p''}{\partial x_j} \right\} = \frac{\partial}{\partial x_j} \left\{ \frac{1}{(\rho C_1 + A_j^{**})} (H_j^{**} - H_j^*) \right\} \quad (6)$$

where

$$H_j^{**} = \sum_{nb} A_k^{**} u_k^{**} + S_j^{**}$$

Correct velocity and pressure

$$(\rho C_1 + A_i^{**}) u_i'' = H_i^{**} - H_i^* - \frac{\partial p''}{\partial x_i} \quad (7)$$

$$u_i^n = u_i^{**} + u''_i \quad (8)$$

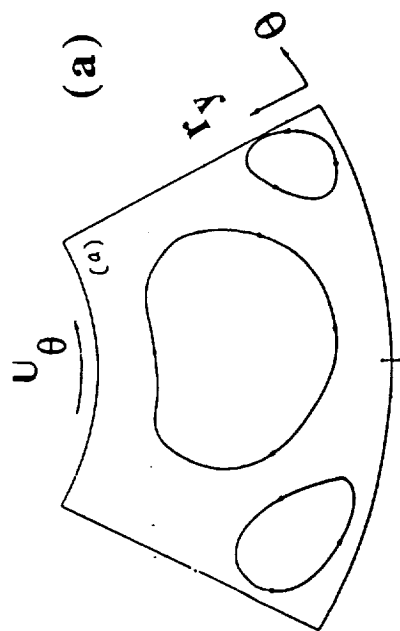
$$p^n = p^* + p'' \quad (9)$$

Solve eqs. (1-9) for each time-level.

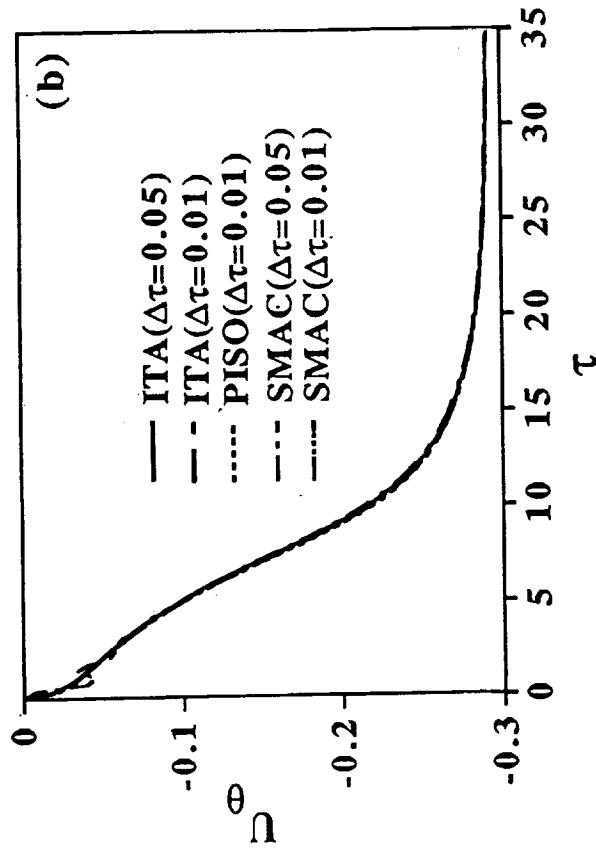
In the 2nd corrector step, the velocity and pressure are driven by the momentum imbalance.

The velocity field may not satisfy the conservation of mass accurately.

Consequently, the conservation of momentum can not be satisfied accurately if a large mass imbalance occur.

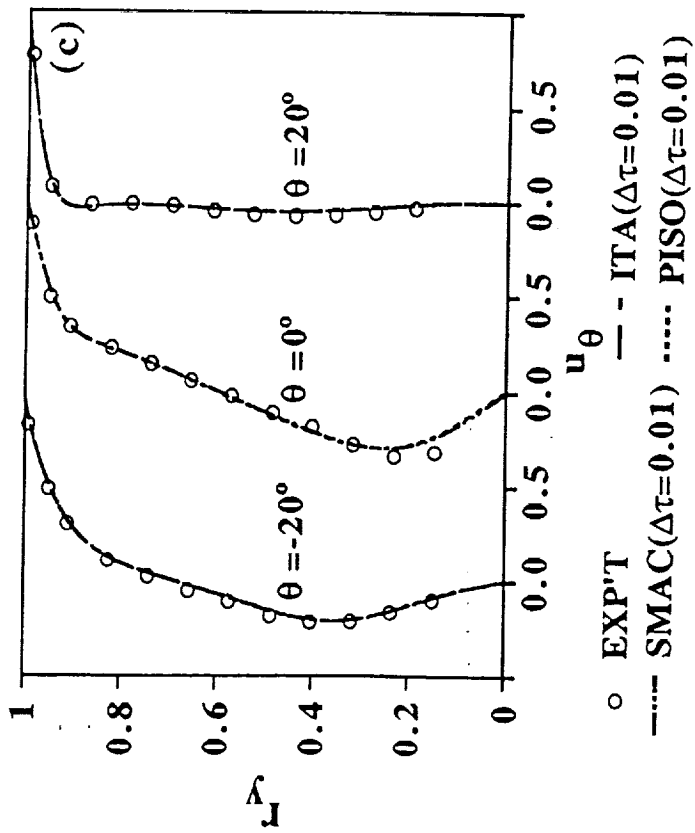


(a) nomenclature

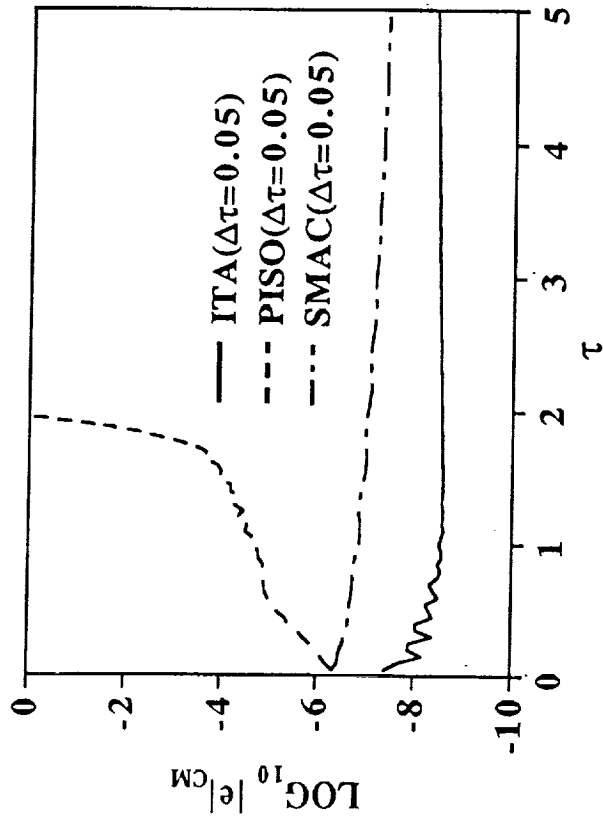


(b) evolution of u_θ at $(r_y, \Theta) = (0.246, 0)$

Polar cavity flow starting from rest

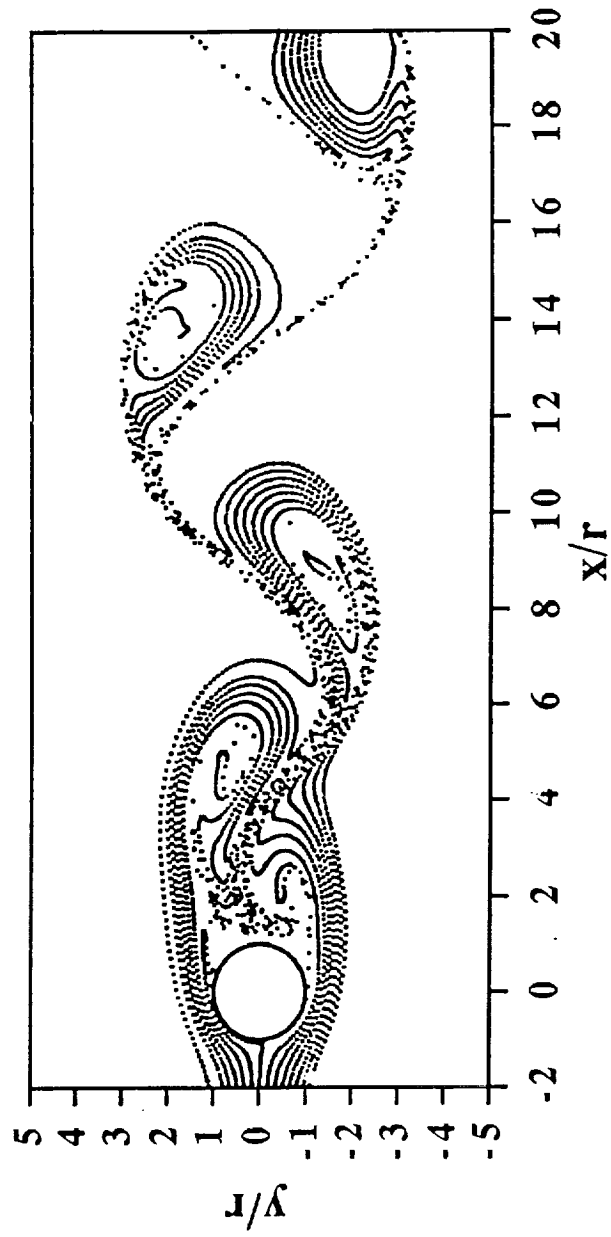


(c) u_θ velocity profiles

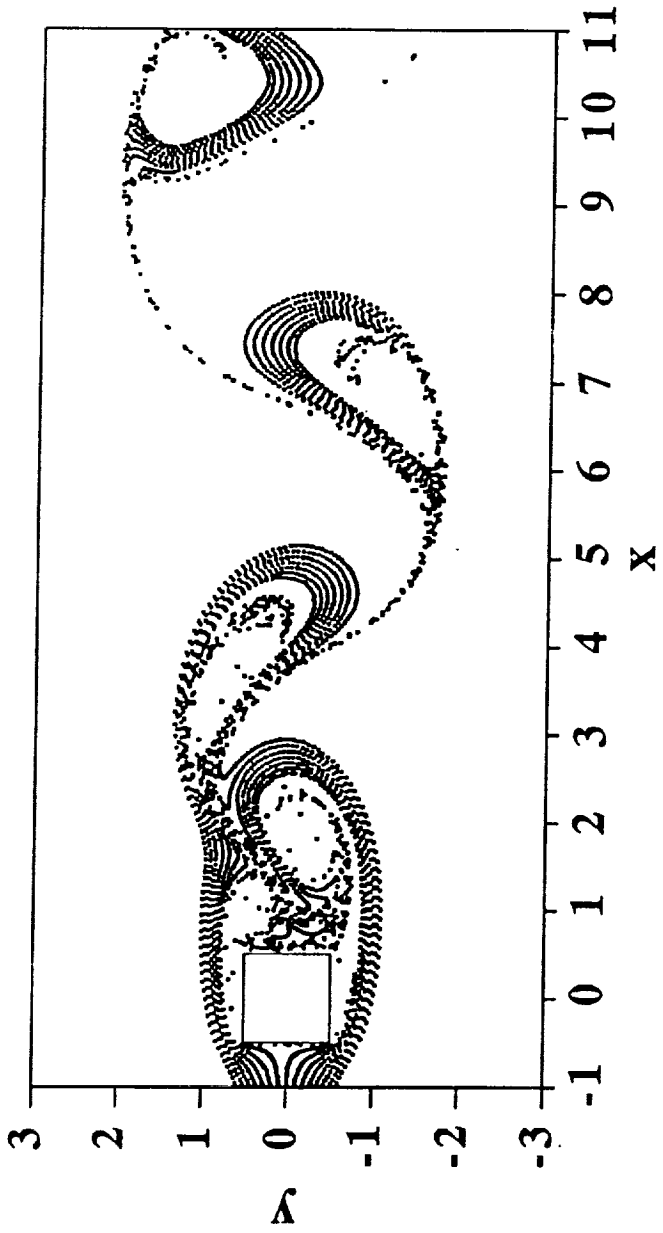


(d) mass imbalance

Polar cavity flow starting from rest



Streaklines for flow over a circular cylinder.



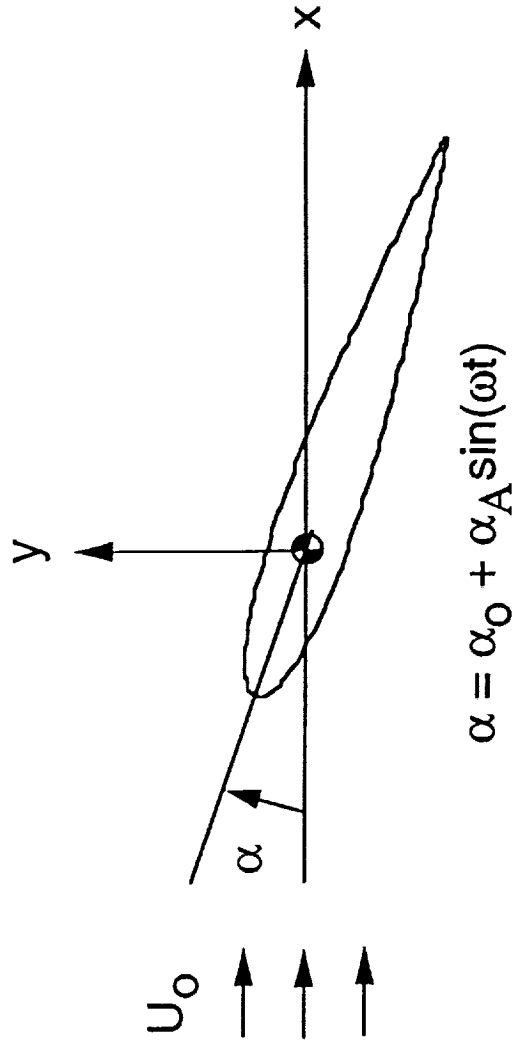
Streamlines for flow over a square cylinder.

Strouhal Numbers ($St = 2fr/U_0$) for Flow over a Circular Cylinder

	ITA		SMAC		PISO		Ref. [2]	Ref. [14]	Exp' t
$\Delta\tau$	0.05	0.05	0.01	0.05	0.01	0.01	0.01	—	—
S_t	0.158	0.155	0.157	0.164	0.160	0.16	0.147	0.16	0.16

Ref. [2]: Braza, Chassing, Ha Minh, JFM 1986,
 Ref. [14]: Eaton, JFM 1987.

Calculation of Unsteady Transitional Flow over Oscillating Airfoil*



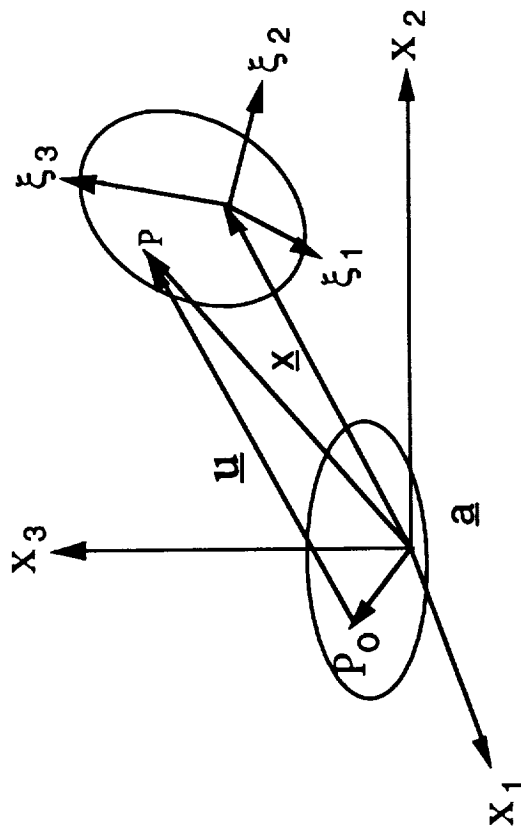
α : angle of attack

α_0 : mean angle of attack ($=15^\circ$)

α_A : amplitude of oscillation ($=10^\circ$)

ω : angular velocity ($=2\pi f$, $f=3.924\text{Hz}$)

* Kim, Zaman, and Panda, To be presented in the ASME Fluid Engineering Conference, Washington D.C., June 20-24, 1993.



Lagrangian-Eulerian coordinates

\mathbf{x} : fixed reference coordinates

ξ : moving coordinates

$$J = |\partial \xi_j / \partial a_j|$$

Conservation of mass equation

$$\frac{\partial}{\partial t}(\rho J) = J \frac{\partial}{\partial x_j} \left\{ \rho (u_j^g - u_j) \right\} \quad (1)$$

Conservation of linear momentum equation

$$\frac{\partial}{\partial t}(\rho u_i J) = J \frac{\partial}{\partial x_j} \left\{ \rho u_i (u_j^g - u_j) \right\} + J \frac{\partial \tau_{ij}}{\partial x_j} - J \frac{\partial p}{\partial x_i} \quad (2)$$

Convection-diffusion equation for scalar variables (i.e., $\phi = \{k_p, \varepsilon_p, k_t, \varepsilon_t, \text{etc.}\}$)

$$\frac{\partial}{\partial t}(\rho \phi J) = J \frac{\partial}{\partial x_j} \left\{ \rho \phi (u_j^g - u_j) \right\} + J \left\{ \mu_e \frac{\partial \phi}{\partial x_j} \right\} - J \rho f(\phi)$$

Ensemble average

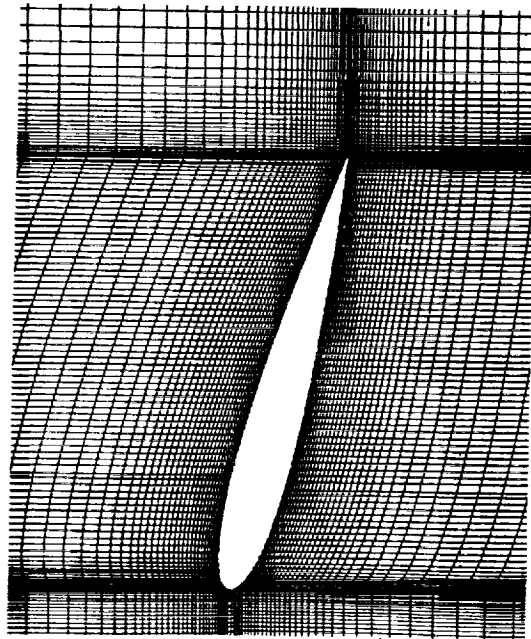
$$\bar{u}(x_0, t_0) = \lim_{N \rightarrow \infty} \left\{ \frac{1}{N} \sum_{n=1}^N u(x_0, t_0) \right\}$$

Aside: Time average

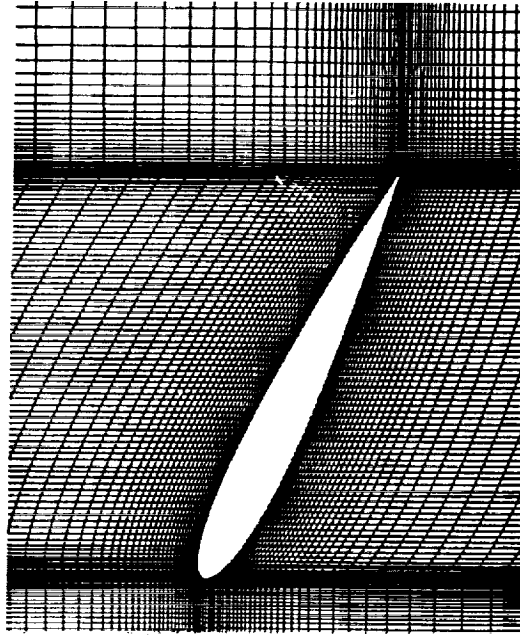
$$\mathbf{u} = \bar{\mathbf{u}} + \mathbf{u}'$$

$$\bar{u} = \lim_{T \rightarrow \infty} \left\{ \frac{1}{T} \int_{t_0}^{t_0+T} u \, dt \right\}$$

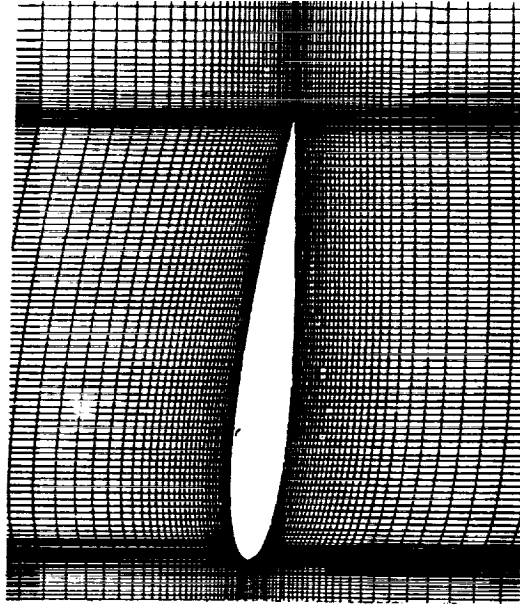
Hence $\frac{\partial \bar{u}}{\partial t} = 0$, and the time-average is useful for steady flows only.



(a) $\alpha = 15^\circ$, $t/\Gamma = 0.0$

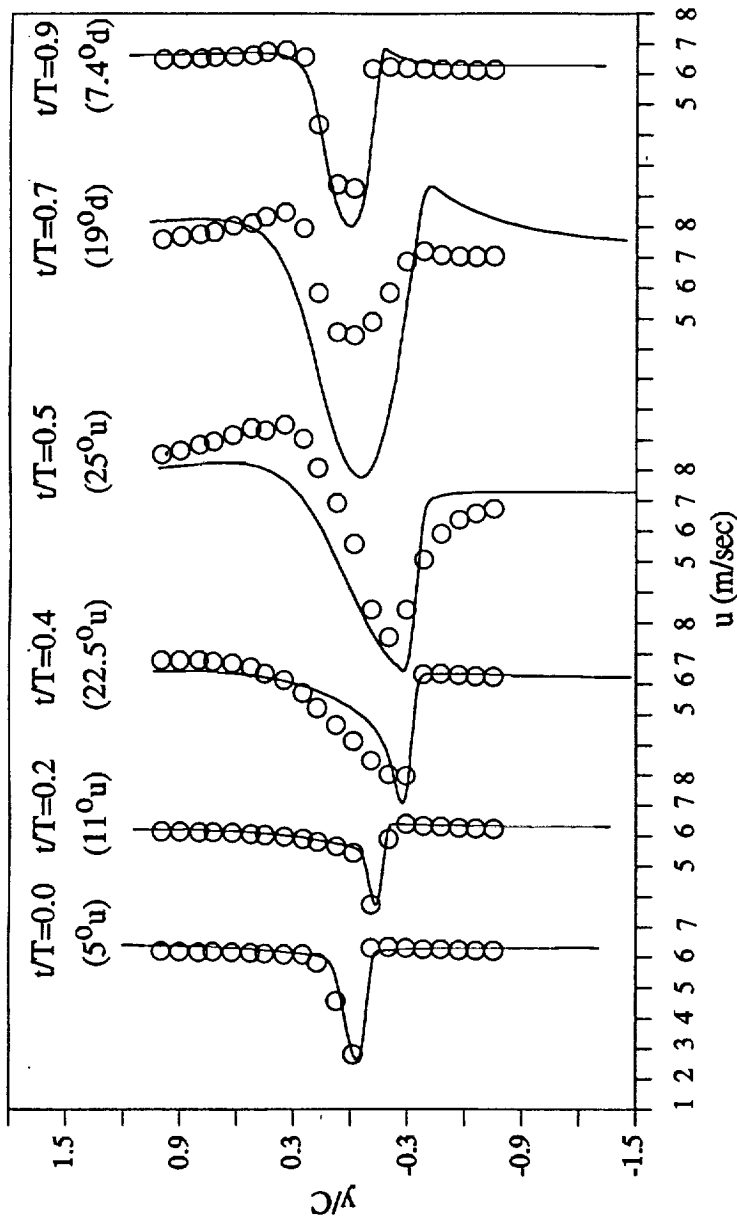


(b) $\alpha = 25^\circ$, $t/\Gamma = \pi/2$



(c) $\alpha = 50^\circ$, $t/\Gamma = 3/2 \pi$

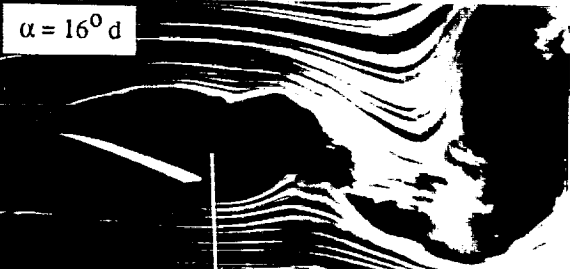
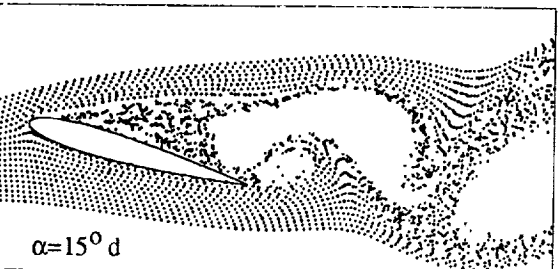
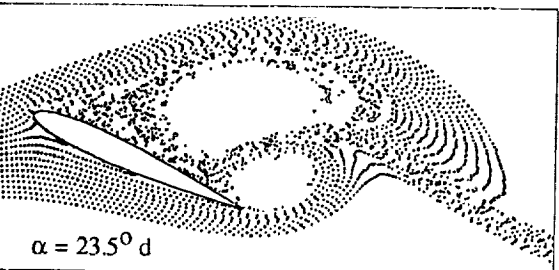
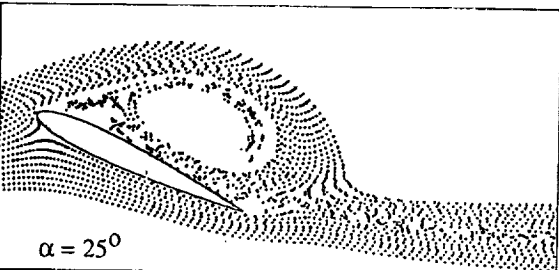
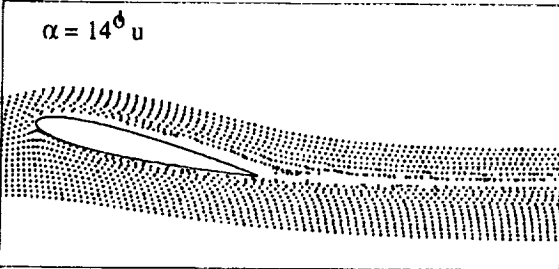
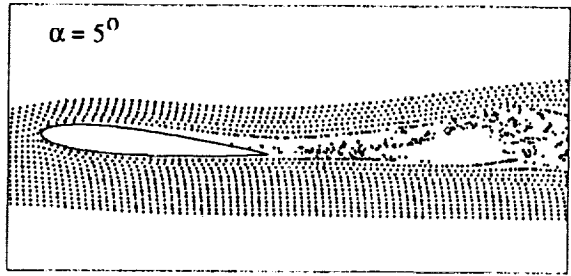
Oscillating airfoil and moving mesh



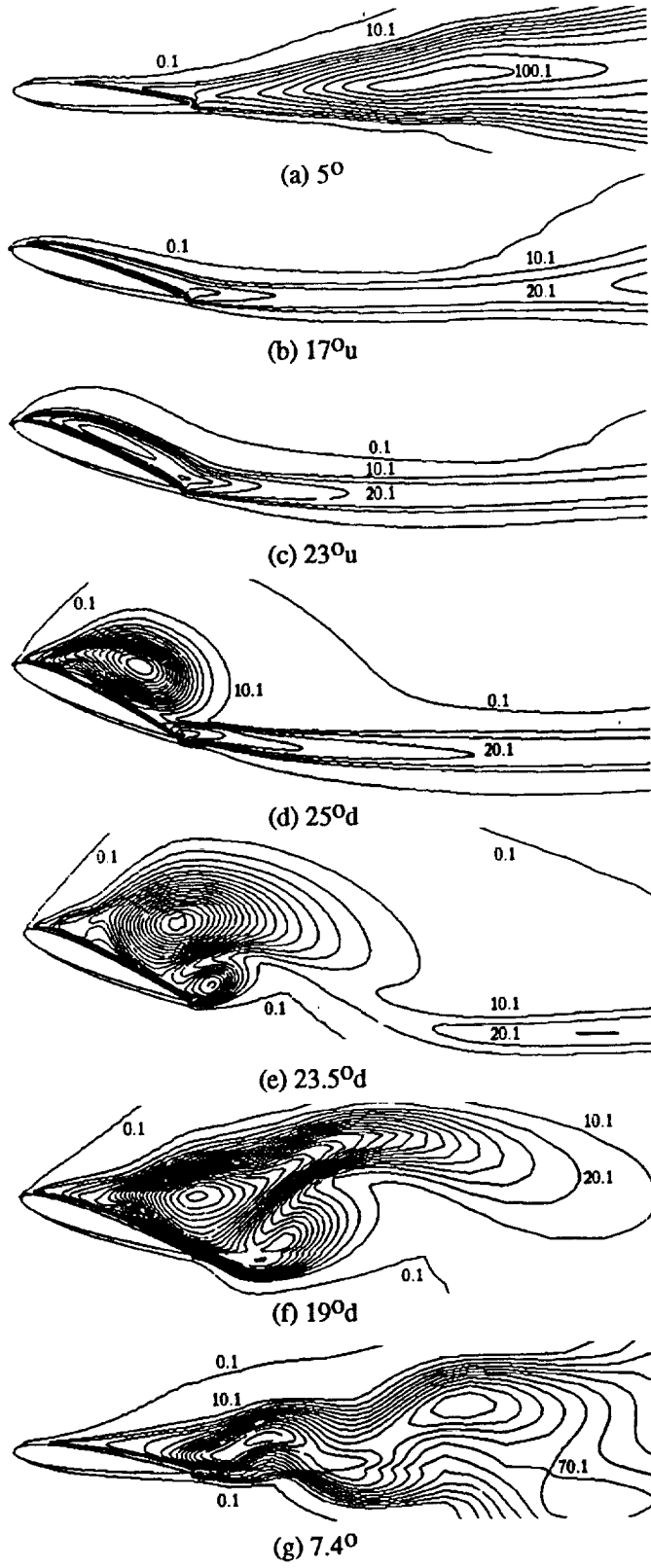
Ensemble-averaged velocity profiles at $x/c=1.0$

The deteriorated comparison at $\alpha \approx 19^\circ$ d

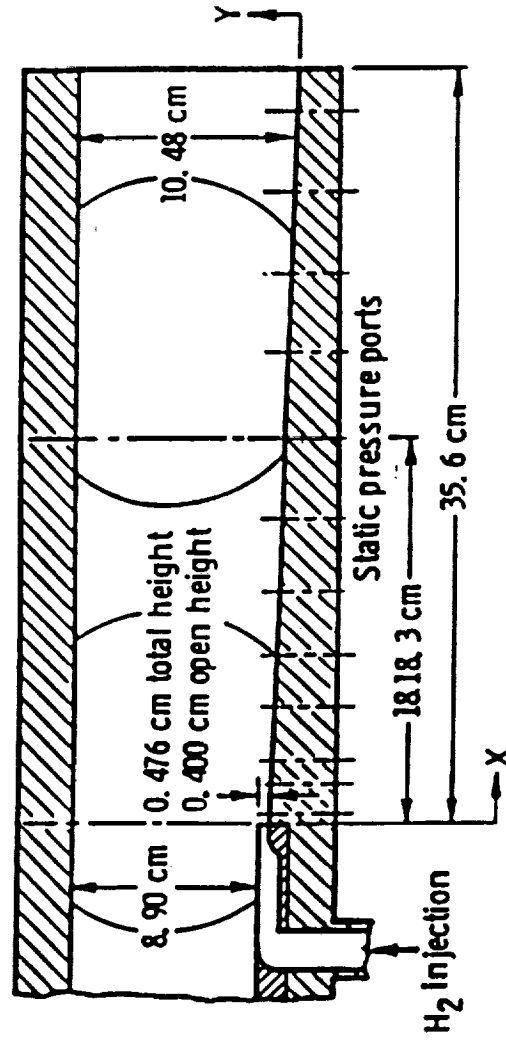
- (i) The hot wire can not accurately measure the velocity components when the flow is misaligned more than approximately 30° from the hot wire axis.
- (ii) The interaction between the DSV and the TEV occurs in a relatively coarse mesh region and the numerical method yields somewhat deteriorated results.



Comparison of calculated streaklines with smoke picture.



Turbulent viscosity contour ($\Delta\mu/\mu_t = 10$)



Combustion of H₂ in vitiated supersonic airstream (Burrows and Kurkov, 1973)

Chemical species concentration equation

$$\frac{\partial}{\partial t} (\rho Y_i) + \nabla \cdot (\rho Y_i (\mathbf{v} + \mathbf{V}_i)) = \dot{w}_i$$

where the diffusion velocity, \mathbf{V}_i , is approximated using the Fick's law given as

$$\mathbf{V}_i \mathbf{V}_i = - (D_{i,1} + D_{i,t}) \nabla Y_i$$

The production rate of the i -th species, \dot{w}_i , is given as

$$\dot{w}_i = \sum_{k=1}^{N_r} M_i (n_{i,k}'' - n_{i,k}') w_k$$

where

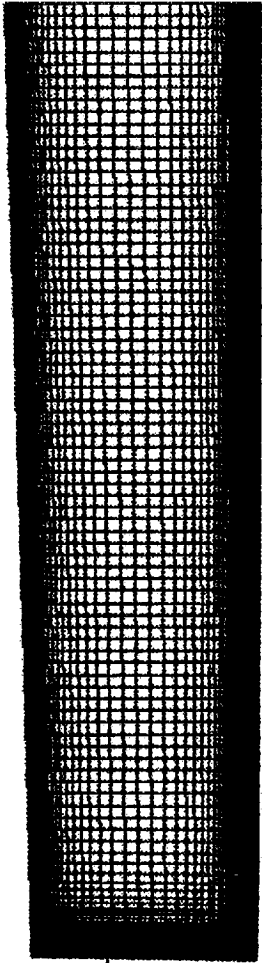
$$w_k = k_{f,k} \prod_{j=1}^{N_s} c_j^{v_{j,k}'} - k_{b,k} \prod_{j=1}^{N_s} c_j^{v_{j,k}''}$$

Chemical reactions for the combustion of H_2 in a vitiated supersonic airstream are described using 9 chemical species (H_2 , O_2 , H_2O , OH , O , H , HO_2 , H_2O_2 , and N_2) and 48 reaction-steps (Burks and Oran, 1981; Kumar, 1989).

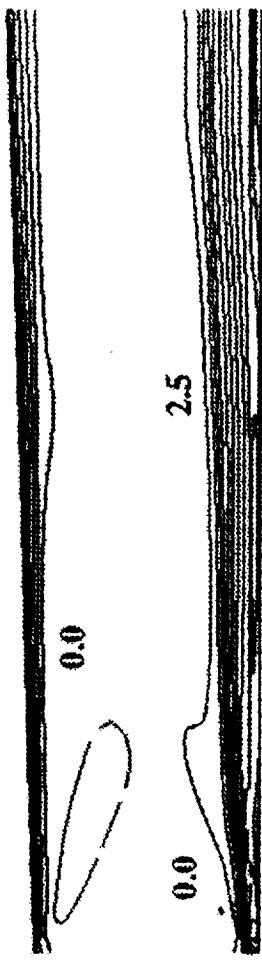
A fast chemistry can not be used to describe the fine details (such as the instability) of chemically reacting flows.

A reduced chemical kinetics can not be used confidently due to the uncertainty contained in the reaction mechanisms.

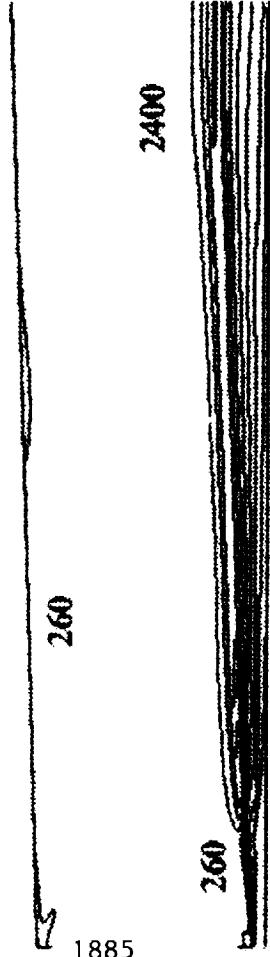
The use of a detailed finite rate chemistry may make it difficult to obtain a fully converged solution due to the coupling between the large number of flow, turbulence, and chemical equations. The numerical method needs to be strongly convergent. Accuracy also depends on the capability of turbulence equations used.



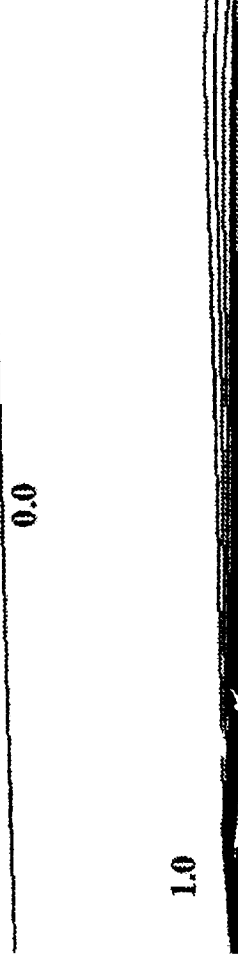
127 x 124 mesh



Mach number contour (dM=0.2)



temperature contour (dT=200)



H2 mass fraction (dY=0.1)

Combustion of H₂ in vitiated supersonic airstream

CONCLUSIONS AND DISCUSSION

On comparison of SMAC, PISO, and ITA

1. The SMAC is the most efficient computationally and yields accurate numerical results.

Calculation of steady flows using an unsteady flow solver.

- * No unsteady flow solver is more efficient than steady flow solvers to solve steady flows (Jang et al., *Numer. Heat Transfer*, 1986.)
- * Only the SMAC can compete with steady flow solvers (ITA with $\Delta\tau=\infty$) to solve steady flows.

2. The 2nd corrector step of PISO.

Velocity and pressure are driven by momentum imbalance. Thus the velocity field is not divergence free. Large amount of mass imbalance can cause divergence.

3. The ITA can best resolve the nonlinearity of the Navier-Stokes Equations.

CONCLUSIONS AND DISCUSSION

Calculations of
incompressible and compressible flows,
steady and unsteady flows,
laminar, transitional, and turbulent flows,
chemically reacting flows
are presented.

Calculations of
chemically reacting flows with spray combustion
Hypersonic Flows.
are in progress.

The accurate numerical results are attributed to the capability of

- (i) the ITA that can best resolve the nonlinearity of the Navier-Stokes equations,
- (ii) the new pressure correction algorithm that can strongly enforce the conservation of mass, and
- (iii) the Multiple-time-scale turbulence equations that can resolve the in-equilibrium turbulence field.

